Biomol NMR Assign (2013) 7:193–197
DOI 10.1007/s12104-012-9408-8

ARTICLE

^{1}H, ^{13}C and ^{15}N resonance assignments and peptide binding site chemical shift perturbation mapping for the *Escherichia coli* redox enzyme chaperone DmsD

Charles M. Stevens · Mark Okon · Lawrence P. McIntosh · Mark Paetzel

Received: 13 February 2012 / Accepted: 21 June 2012 / Published online: 6 July 2012

Abstract Herein are reported the mainchain ^{1}H, ^{13}C and ^{15}N chemical shift assignments and amide ^{15}N relaxation data for *Escherichia coli* DmsD, a 23.3 kDa protein responsible for the correct folding and translocation of the dimethyl sulfoxide reductase enzyme complex. In addition, the observed amide chemical shift perturbations resulting from complex formation with the reductase subunit DmsA leader peptide support a model in which the 44 residue peptide makes extensive contacts across the surface of the DmsD protein.

Keywords DmsD · DmsA · Leader peptide · Protein-peptide complex · Chaperone · Chemical shift perturbation mapping

Introduction and biological context

The twin arginine translocase (Tat) is a means by which fully folded proteins, many with redox sensitive cofactors, are translocated across the plasma membrane of bacteria (Weiner et al. 1998). Substrates for Tat contain a characteristic S/T-R-R-X-F-L-K motif near the N-terminus of their leader peptide sequences (Berks 1996). The substrate proteins themselves are functionally diverse and include virulence factors, transmembrane proteins, lipoproteins and redox enzymes (Lee et al. 2006). Many of these proteins require the involvement of specialized chaperones to ensure their correct folding and assembly prior to translocase targeting (Genest et al. 2009). These chaperones are collectively referred to as redox enzyme chaperone proteins (REMPs) (Turner et al. 2004). The two best studied bacterial REMPs are DmsD and TorD (Oresnik et al. 2001; Pommier et al. 1998). Although a wealth of structural information is available for each, including X-ray crystal structures of DmsD from *Escherichia coli* and TorD from *Shewanella masillia* (Ramasamy and Clemons 2009; Stevens et al. 2009; Tranier et al. 2003), the molecular details of how these REMPs perform their functions remain largely unknown. Despite many studies exploring the interaction of DmsD with the leader peptide from the DmsA subunit of dimethyl sulfoxide reductase. This includes the identification and biochemical characterization of several residues that may play a role in binding and a molecular dynamics simulation with a de novo generated peptide (Chen et al. 2008; Stevens et al. 2009; Winstone et al. 2006), a complete picture of the interactions between DmsD and its substrates has not yet been revealed.

In this note, we report the chemical shift assignments of the mainchain ^{1}H, ^{15}N and ^{13}C nuclei and amide relaxation data for *E. coli* DmsD, as well as a comparison of spectra collected for the chaperone in the presence and absence of the DmsA leader peptide ($DmsA_L$). These data both support the proposed peptide-binding interface of DmsD as a shallow groove extending around the surface of the protein and open the door for future NMR spectroscopic experiments to probe the function of DmsD and elucide its role in the secretion of the DmsABC complex.

C. M. Stevens · M. Paetzel (✉)
Department of Molecular Biology and Biochemistry, Simon Fraser University, 8888 University Drive, Burnaby, BC V5A 1S6, Canada
e-mail: mpaetzel@sfu.ca

M. Okon · L. P. McIntosh (✉)
Department of Biochemistry and Molecular Biology, Department of Chemistry, and the Michael Smith Laboratories, The University of British Columbia, Life Sciences Centre, 2350 Health Sciences Mall, Vancouver, BC V6T 1Z3, Canada
e-mail: mcintosh@chem.ubc.ca

Methods and experiments

The *dmsD* gene from *E. coli* was cloned into the pET-15b expression vector and transformed into BL21(DE3) cells. A 100 mL culture of these cells was grown in Luria broth with ampicillin overnight at 30 °C. The bacteria were harvested by centrifugation at 5,000×*g*, resuspended in 1 L of unlabeled M9 minimal media, grown at 37 °C for 7 h to $OD_{600} = 0.9$, harvested again by centrifugation, and finally resuspended in 300 mL of 99 % D_2O M9 minimal media with 1 g $^{15}NH_4Cl$ and 1 g $^{2}H_7/^{13}C_6$-glucose. After 1 h of incubation at 25 °C, isopropyl-β-thiogalactoside (IPTG, 0.1 mM final) was added to the culture, followed by growth overnight at 25 °C. The His_6-tagged DmsD protein was purified using Ni^{2+}-NTA affinity chromatography (Qiagen), as outlined previously (Stevens et al. 2009). However, to ensure amide protonation, the bound protein was unfolded by treatment with 5 column volumes of TBS (20mM Tris-HCl pH 8.0; 100 mM NaCl) supplemented with 8 M urea and refolded by incubation with 10 column volumes of TBS for 30 min. prior to elution from the affinity column. Further purification to homogeneity was achieved using size exclusion chromatography on a Sephacryl S-100 column, equilibrated with TBS and run with a flow rate of 1.0 mL/min using an ÄKTA prime system. The purified $^{2}H/^{15}N/^{13}C$-labeled protein, containing the full 204 residues of wild type DmsD (UniProt P69853) and a 19 residue N-terminal extension, comprised of a His_6 tag and thrombin protease recognition site (MGSHHHHHHSSGLVPRGSH), was concentrated to 0.8 mM in 50 mM sodium phosphate buffer at pH 6.5 with 5 % D_2O using a 10 kDa MWCO Amicon centrifugal filter (Millipore). A non-deuterated $^{15}N/^{13}C$-labeled sample was prepared as above using H_2O M9 media and $^{13}C_6$-glucose.

A complex of labeled DmsD with the unlabeled $DmsA_L$ leader peptide (residues 1–44 of DmsA followed by a proline, a thrombin protease cleavage site, and a His_6- tag) was obtained as described previously (Stevens and Paetzel 2012). Note that $DmsA_L$ must be co-expressed and co-purified with DmsD. Thus $^{2}H/^{15}N/^{13}C$-labeled DmsD was exchanged for unlabeled DmsD while the $DmsA_L$ was immobilized on a Ni^{2+}-NTA affinity column. After elution with imidazole, the desired sample was concentrated to 5 mL and applied to a Sephacryl S-100 column, equilibrated with 50 mM sodium phosphate buffer at pH 6.5, and run with a flow rate of 1.0 mL/min. Resolved fractions containing the complex of unlabeled $DmsA_L$ and $^{2}H/^{13}C/^{15}N$-labeled DmsD were concentrated to 400 μM in 50 mM sodium phosphate buffer at pH 6.5 using a 10 kDa MWCO Amicon centrifugal filter.

NMR spectra were recorded at 25 °C using a Bruker 850 MHz Avance III spectrometer equipped with a $^{1}H/^{13}C/^{15}N$ TCI cryoprobe. The spectra were processed with NMRPipe (Delaglio et al. 1995) and analyzed with Sparky (Goddard and Kneller 2008). External 2,2-dimethyl-2-siliapentane-sulfonic acid (DSS) was used as a direct reference for ^{1}H and indirect for ^{13}C and ^{15}N. The signals from the mainchain nuclei of $^{2}H/^{13}C/^{15}N$-labeled DmsD at pH 6.5 were assigned using ^{2}H-decoupled TROSY-based ^{15}N-HSQC, HNCO, HN(CA)CO, HNCACB, HN(CO)-CACB, and non-TROSY C(CO)-TOCSY-NH spectra (Sattler et al. 1999), combined with 150 ms mixing time 3D ^{1}H- and ^{15}N-resolved NOESY-HSQC spectra (Ikura et al. 1990). Amide ^{15}N heteronuclear NOE relaxation data for a non-deuterated sample of $^{15}N/^{13}C$-labeled DmsD were recorded with a 600 MHz Varian Inova spectrometer (Farrow et al. 1994).

Amide $^{1}H^{N}$ and ^{15}N assignments for labeled DmsD in complex with unlabeled $DmsA_L$ at pH 6.5 were assigned from ^{2}H-decoupled TROSY-based HNCACB and HNCA (CO)CB spectra, using the spectra for the free protein as a guide. The chemical shift perturbation for each residue with assigned signals in the spectra of both free and complexed DmsD was calculated as $\Delta\delta = [(\Delta\delta_{1H})^2 + (\Delta\delta_{15N}/5)^2]^{1/2}$.

Results and discussion

Overall, DmsD yielded a ^{15}N-HSQC spectrum with excellent dispersion and lineshape, indicating that this 23.3 kDa protein is stably folded and well behaved in solution (Fig. 1a). Assignment of signals from main chain $^{1}H^{N}$, ^{15}N, $^{13}C^{\alpha}$, $^{13}C^{\beta}$ and/or $^{13}C'$ nuclei were obtained for 166 of 190 non-proline residues using standard triple resonance approaches and have been deposited in the BioMagResBank (http://www.bmrb.wisc.edu) with accession number 18257. Signals from residues 4–9, 16, 74–78, 87–88, 97, 128–131, and 153 could not be assigned unambiguously, most likely due to spectral overlap. A second set of weaker $^{1}H^{N}$-^{15}N peaks was also identified for 63 residues broadly clustering near helix 5. The origin of this conformational heterogeneity is unclear as this region is lacking in prolines and, although containing an exposed cysteine, addition of excess DTT did not alter the spectra of DmsD. Parenthetically, although deuteration and the use of a 850 MHz NMR spectrometer with TROSY-based pulse sequences improved the quality of the DmsD spectra, a total of 161 assignments, including those from duplicate peaks, were obtained from data recorded for an initial $^{15}N/^{13}C$-labeled sample of the protein using a 600 MHz spectrometer.

The secondary structural elements of DmsD derived from main chain ^{13}C chemical shifts using the SSP (Marsh et al. 2006) and MICS (Shen and Bax 2012) algorithms (Fig. 1b) are in good agreement with those observed in the X-ray crystallographic model of the helical protein

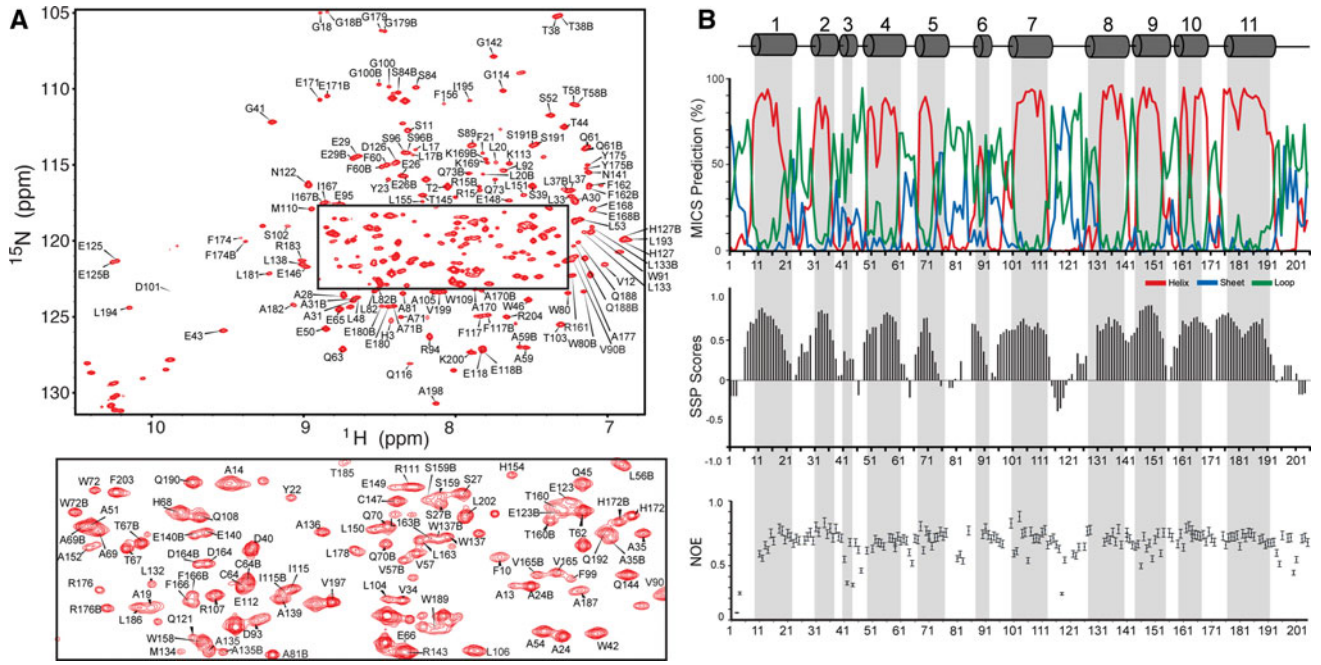

Fig. 1 **a** Assigned ^{15}N-HSQC TROSY spectrum of DmsD (pH 6.5, 25 °C). Backbone ^{1}H^{N}-^{15}N peaks are labeled by residue and the boxed region is expanded in the additional panel. 'B' denotes the weaker peak for amides yielding two signals. **b** *Top* Confidence scores for the predicted secondary structure as helix (*red*), loop (*green*) and strand (*blue*) generated from main chain chemical shifts by the MICS program (Shen and Bax 2012). *Middle* Secondary structure propensity (SSP) scores based on backbone $^{13}C^{\alpha}$, $^{13}C^{\beta}$, $^{13}C'$ chemical shifts (Marsh et al. 2006). Values approaching +1 and −1 are diagnostic of α-helical and *β*-strand conformations, respectively. *Lower* Amide heteronuclear ^{15}N-NOE values for DmsD. Blank points correspond to unassigned amides and prolines. Reduced NOE values, indicative of increased sub-nanosecond timescale motions, are observed at the termini and the loops between helices 5 and 6 and between helices 7 and 8. The *cylinders* denote α-helices observed in the X-ray crystallographic structure of DmsD (PDB: 3EFP) (Stevens et al. 2009)

(PDB: 3EFP and 3CW0) (Ramasamy and Clemons 2009; Stevens et al. 2009). However, some small differences are observed, such as the indication from chemical shifts of *β*-strand character in the flexible loop region between helices 7 and 8. The SSP, but not MICS, algorithm also suggests that helices 10 and 11 extend longer than observed within the crystallized protein.

Insights into the local backbone dynamics of DmsD are provided by the steady-state heteronuclear ^{15}N NOE values shown in Fig. 1b. In general, the backbone of the protein is well ordered, with enhanced fast timescale flexibility only observed in the loop regions between helices 5 and 6 and between helices 7 and 8. The former contribute to the proposed binding site for the DmsA leader peptide (Chan et al. 2008; Stevens et al. 2009), and the latter comprises the hinge region between two subdomains of the protein that is flexible in the X-ray crystal structures of all of the TorD-like REMP proteins (Stevens et al. 2009; Tranier et al. 2003; Ramasamy and Clemons 2009).

To investigate the mechanism of leader peptide binding, a complex of unlabeled $DmsA_L$ and ^{2}H/^{13}C/^{15}N-labeled DmsD was prepared. As shown in Fig. 2, the ^{15}N-HSQC TROSY spectra of free and bound DmsD differ significantly. Unfortunately, titration experiments to aid spectral assignments were not possible as $DmsA_L$ binds with 0.2 μM affinity (Winstone et al. 2006) and is not soluble in isolation. Although the spectra of the complex were of poorer quality than those of the free protein, we were able to confidently assign signals from 160 amides and thereby obtain chemical shift perturbations due to peptide binding. When mapped onto the structure of free DmsD, amides showing the greatest chemical shift perturbations cluster to one broad surface region (Fig. 2b, c). This region overlaps, in part, with residues (18, 72, 75, 76, 86, 87, 123, 124, 126, 127, 147, 151, and 172) shown previously by mutagenesis to be important for leader peptide binding (Chan et al. 2008). Some discrepancies between the two approaches arise, possibly due to indirect effects of mutations and incomplete spectral assignments for the complex. For example, residues 72, 126, 127, 150, and 172 did not undergo large chemical shift perturbations, even though they were shown to be important by mutagenesis. Additionally, perturbations for Pro86, Pro124, and the unassigned Glu123 could not be assessed by these NMR methods despite being identified in the previous mutagenesis study. Nevertheless, these data are consistent with the hypothesis that $DmsA_L$ binds DmsD along a hydrophobic surface groove that extends from the previously identified

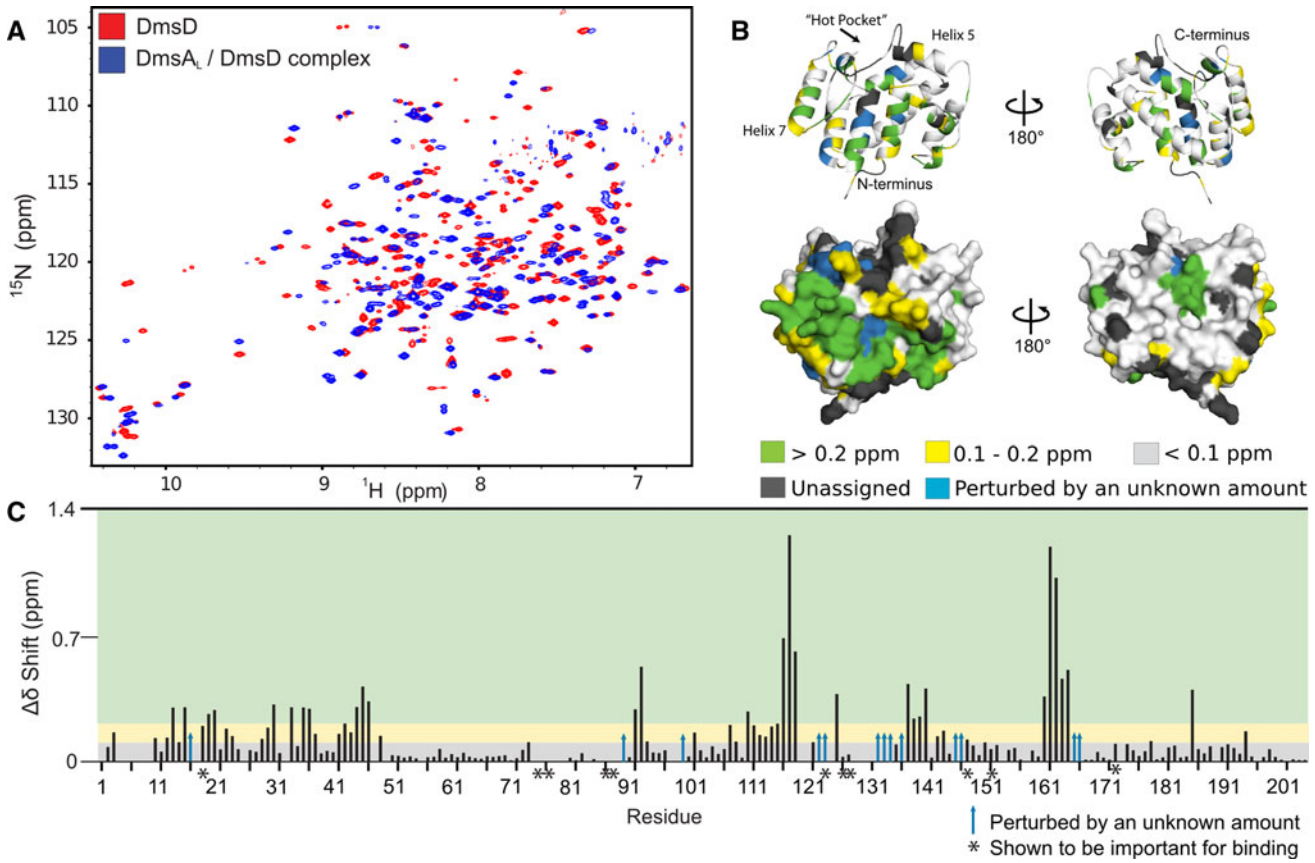

Fig. 2 **a** Superimposed ^{15}N-HSQC TROSY spectra of DmsD in the absence (*red*) and presence of unlabeled DmsA$_L$ (*blue*). **b**, **c** Chemical shift perturbations $\Delta\delta$ for amides with assigned signals in both forms of DmsD are mapped onto a ribbon and surface diagram of free DmsD (PDB: 3EFP) with the indicated *color code*. In **c**, blank points correspond to prolines and unassigned amides in the free protein, and an average shift was used for residues with two signals. In **b** and **c**, *blue arrows* and *blue surface regions* indicate residues that were assigned in the free DmsD and have a perturbed, albeit unassigned, chemical shift in the complex. Residues shown previously to be important for binding by mutagenesis are highlighted by an *asterisk* (Chan et al. 2008)

"hot pocket" between helices 5, 6, and 7 (Chan et al. 2008) outward across the "front" surface of the protein toward helices 3 and 4 (Fig. 2c left), as well as towards Arg161 on the "back" face of the protein (Fig. 2c right).

It is also noteworthy that a ^{13}C/^{15}N-filtered NOESY spectrum yielded only signals from the unlabeled peptide with poorly dispersed ^{1}H^N chemical shifts (not shown). This suggests that the DmsA$_L$ leader does not adopt any predominant helical or stand conformation when bound to DmsD. This is similar to what was observed in a previously reported molecular dynamics simulation of leader peptide binding (Stevens et al. 2009), but is in contrast to predictions that the leader peptide adopts a helical conformation upon binding to the REMP (Buchanan et al. 2008).

Acknowledgments The authors would like to acknowledge Eric Escobar, Hyun-Seo Kang and Kelly Kim for assistance with Sparky and assignment techniques and Dr. R. J. Turner for providing the plasmid from which our DmsD construct was cloned. NMR instrument support was provided by the Canadian Institutes for Health Research (CIHR), the Canadian Foundation for Innovation (CFI), the British Columbia Knowledge Development Fund (BCKDF), the UBC Blusson Fund, and the Michael Smith Foundation for Health Research (MSFHR). M. P. acknowledges funding from the National Science and Engineering Research Council of Canada (NSERC), CIHR and MSFHR. L. M. acknowledges funding from NSERC.

References

Berks BC (1996) A common export pathway for proteins binding complex redox cofactors? Mol Microbiol 22:393–404

Buchanan G, Maillard J, Nabuurs SB, Richardson DJ, Palmer T, Sargent F (2008) Features of a twin-arginine signal peptide required for recognition by a Tat proofreading chaperone. FEBS Lett 582:3979–3984

Chan CS, Winstone TML, Chang L, Stevens CM, Workentine ML, Li H, Wei Y, Ondrechen MJ, Paetzel M, Turner RJ (2008) Identification of residues in DmsD for twin-arginine leader peptide binding, defined through random and bioinformatics-directed mutagenesis. Biochemistry 47:2749–2759

Chen S, Fan Y, Shen X, Sun P, Jiang G, Shen Y, Xue W, Li Y, Chen X (2008) A molecular modeling study of the interaction between

SRP-receptor complex and peptide translocon. Biochem Biophys Res Commun 377:346–350

Delaglio F, Grzesiek S, Vuister GW, Zhu G, Pfeifer J, Bax A (1995) NMRPipe: a multidimensional spectral processing system based on UNIX pipes. J Biomol NMR 6:277–293

Farrow NA, Muhandiram R, Singer AU, et al (1994) Backbone dynamics of a free and phosphopeptide-complexed Src homology 2 domain studied by ^{15}N NMR relaxation. Biochemistry 33:5984–6003

Genest O, Méjean V, Iobbi-Nivol C (2009) Multiple roles of TorD-like chaperones in the biogenesis of molybdoenzymes. FEMS Microbiol Lett 297:1–9

Goddard TD, Kneller DG (2008) SPARKY. University of California, San Fransisco

Ikura M, Bax A, Clore GM, Gronenborn AM (1990) Detection of nuclear Overhauser effects between degenerate amide proton resonances by heteronuclear three-dimensional NMR spectroscopy. J Am Chem Soc 112(24):9020–9022

Lee PA, Tullman-Ercek D, Georgiou G (2006) The bacterial twin-arginine translocation pathway. Annu Rev Microbiol 60:373–395

Marsh JA, Singh VK, Jia Z, Forman-Kay JD (2006) Sensitivity of secondary structure propensities to sequence differences between alpha- and gamma-synuclein: implications for fibrillation. Protein Sci 15:2795–2804

Oresnik IJ, Ladner CL, Turner RJ (2001) Identification of a twin-arginine leader-binding protein. Mol Microbiol 40:323–331

Pommier J, Méjean V, Giordano G, Iobbi-Nivol C (1998) TorD, a cytoplasmic chaperone that interacts with the unfolded trimethylamine N-oxide reductase enzyme (TorA) in *Escherichia coli*. J Biol Chem 273:16615–16620

Ramasamy SK, Clemons WM (2009) Structure of the twin-arginine signal-binding protein DmsD from *Escherichia coli*. Acta Crystallogr Sect F 65:746–750

Sattler M, Schleucher J, Griesinger C (1999) Heteronuclear multidimensional NMR experiments for the structure determination of proteins in solution employing pulsed field gradients. Prog Nucl Magn Reson Spectrosc 34:93–158

Shen Y, Bax A (2012) Identification of helix capping and b-turn motifs from NMR chemical shifts. J Biomol NMR 52(3):211–232

Stevens CM, Paetzel M (2012) Purification of a Tat leader peptide by co-expression with its chaperone. Protein Expr Purif 84(1):167–172

Stevens CM, Winstone TML, Turner RJ, Paetzel M (2009) Structural analysis of a monomeric form of the twin-arginine leader peptide binding chaperone *Escherichia coli* DmsD. J Mol Biol 389: 124–133

Tranier S, Iobbi-Nivol C, Birck C, Ilbert M, Mortier-Barrière I, Méjean V, Samama J-P (2003) A novel protein fold and extreme domain swapping in the dimeric TorD chaperone from *Shewanella massilia*. Structure 11:165–174

Turner RJ, Papish AL, Sargent F (2004) Sequence analysis of bacterial redox enzyme maturation proteins (REMPs). Can J Microbiol 50:225–238

Weiner JH, Bilous PT, Shaw GM, Lubitz SP, Frost L, Thomas GH, Cole JA, Turner RJ (1998) A novel and ubiquitous system for membrane targeting and secretion of cofactor-containing proteins. Cell 93:93–101

Winstone TL, Workentine ML, Sarfo KJ, Binding AJ, Haslam BD, Turner RJ (2006) Physical nature of signal peptide binding to DmsD. Arch Biochem Biophys 455:89–97